Pak. J. Agri. Sci., Vol. 58(1), 381-388; 2021
ISSN (Print) 0552-9034, ISSN (Online) 2076-0906
DOI: 10.21162/PAKJAS/21.957
http://www.pakjas.com.pk

GREEN SYNTHESIS OF AG NANOPARTICLES USING LEAF AQUEOUS EXTRACTS OF *Aizoon canariense* L. GROWING IN ASIR, SAUDI ARABIA AGAINST PLANT PATHOGENIC FUNGI

Mahmoud Moustafa[1,2*], Mahmoud Sayed[3,4], Saad Alamri[1,5], Huda Alghamdii[1], Ali Shati[1], Sulaiman Alrumman[1], Mohmed Al-Khatani[1], Thanaa Maghraby[2], Hanan Temerk[2], Eman Khalaf[6] and Sally Negm[7,8]

[1]Department of Biology, College of Science, King Khalid University, 9004, Abha, Kingdom of Saudi Arabia, [2]Department of Botany and Microbiology, Faculty of Science, South Valley University, Qena, Egypt, [3]Department of Physics, Faculty of Science, King Khalid University, Abha, Kingdom of Saudi Arabia, [4]Department of Physics, Faculty of Science, Al-Azhar University, Assiut, Egypt, [5]Prince Sultan Bin Abdulaziz Center For Environmental and Tourism Research and Studies, King Khalid University, Kingdom of Saudi Arabia, [6]Department of Microbiology and Immunology, Faculty of Pharmacy, Damanhour University, Damanhour, Egypt, [7]Department of Life Sciences, College of Science and Literature Mahyel Aseer, King Khalid University, Abha, Kingdom of Saudi Arabia, [8]Unit of Food Bacteriology, Central Laboratory of Food Hygiene, Ministry of Health, Branch in Zagazig, Sharkia, Egypt
***Corresponding author, e-mail: mfmostfa@kku.edu.sa**

It is well known that silver nanoparticles are a good candidate to be antifungal agent against wide range of plant pathogenic fungi. The objective of this work is to examine the impact of silver nanoparticles (AgNPs) synthesized from *Aizoon canariense* L. aqueous fresh leaf extract as antifungal agent. The formation of AgNPs from leaf extracts are confirmed using Fourier Transform Infrared Spectroscopy analysis (FTIR), UV-visible spectrophotometer (UV–visible), X-Ray Diffraction (XRD) and Scanning electron microscopy (SEM). The AgNPs from fresh cold and hot water extracts of *A. canariense* leaf exhibited highest absorption at 444 and 426 nm, respectively, through ultraviolet visible spectroscopy. Fourier transform infrared spectroscopy has verified the transformation of Ag^+ ions to AgNPs owing to the reduction by capping material of aqueous plant extract. The X-RD pattern revealed the presence of crystalline having size ranging from 12.95 to 10.83 nm for cold and hot aqueous extract, respectively, based on FWHM of the diffraction peaks. SEM showed that the synthesized AgNPs are semi spherical with an average size between (42 and 183 nm) for NPs from cold water and (29 and 138 nm) for NPs from hot water extracts based on SMILEVIEW software. The synthesized silver nanoparticles from hot water extract showed higher antifungal action than cold water extract in the range between 10.17 and 19.85% against *Alternaria alternate, Drechslera halodes, Fusarium oxysporum f. sp. lycopersici, Penicillium expansum, Rhizoctonia solani, Pythium ultimum, and Macrophomina phaseolina*. These findings may suggest *A. canariense* aqueous fresh leaf extract could be applied as a natural solution for biosynthesizing AgNPs as eco-friendly antifungal drug against plant pathogenic fungi.
Keywords: *Aizoon canariense*, Antifungal, Asir, Green synthesis, Leaf extract

INTRODUCTION

Nanotechnology is new area of interdisciplinary study which implies the use of materials with nanoscale dimensions. Such structures pose a variety of applications that demonstrated antimicrobial activity and this feature is a crucial tool in combating microorganisms resistant to exciting antibiotics (Shenashen *et al.*, 2014). Nanoparticle discovery is necessary today, not just in terms of application but also in terms of synthesis (Kannan *et al.*, 2010). Silver was considered as a non-toxic, healthy inorganic antibacterial agent which able to kill approximately 650 forms of microorganism-causing diseases (Jeong *et al.*, 2005). Silver nanoparticles are vital components that have been extensively studied, these nanoparticles possess specific electrical, optical and biological properties and thus are used in catalysis, biosensing, imaging, drug delivery, nano-device manufacturing and in medication (Jain *et al.*, 2008; Magudapathy *et al.*, 2001; Moustafa *et al.*, 2018a). Plants are valuable source of several bioactive compounds used to control pests and predators, as well as other plant, human and animal diseases (Alamri and Moustafa, 2012; Alghamdi, 2013; Lin *et al.*, 2000). In addition, plant extract can serve as a reducing and capping agent for nanoparticle synthesis, which is more beneficial than other biological processes (Valli and Vaseeharan, 2012). Furthermore, the use of the green synthesis method by researchers is increasing due to the use of less toxic materials, the eco-friendly design and in one

stage synthesis of required nanoparticles (Valli and Vaseeharan, 2012).

Antibacterial activity of AgNPs against various bacterial strains such as *Pseudomonas aeruginos (Salomoni et al., 2017)*, *Staphylococcus aureus* (MRSA) (Qais *et al.*, 2019), *Streptococcus mutans* and *Escherichia fergusonii* (Gurunathan, 2019), etc, has been reported. Studies have also explored the effectiveness of AgNPs to control plant fungal pathogens such as *Alternaria alternate*, *Alternaria brassicicola, Alternaria solani, Cladosporium cucumerinum, Botrytis cinerea*, *Corynespora cassiicola*, *Cylindrocarpon destructans*, *Didymella bryoniae*, *Fusarium* spp., *Monosporascus cannonballus*, *Glomerella cingulate*, *Pythium* spp., and *Stemphylium lycopersici* (Kim *et al.*, 2012). Likewise, the effective removal of sclerotium-forming fungi was accomplished in a dose-dependent manner once silver nanoparticles (AgNPs) were used (Min *et al.*, 2009).

Instead to chemical synthetic fungicides, the use of silver nanoparticles as antifungal agents is becoming more popular as a new technical developments have made their processing easier and economical (Jo *et al.*, 2009). Silver exhibited several forms of inhibiting action against various pathogenic microorganisms (Clement and Jarrett, 1994); then, it is worth to be applied it with relative safety to control various plant pathogens compared to other conventional fungicides (Park *et al*., 2006).

Despite arid climate condition of Saudi Arabia, the flora in the southern part of the country is rich owing to the unique geographical location including high elevation which indirectly affects the rate of precipitation, humidity and temperature etc. As a results about 70% of the plant species growing in Saudi Arabia have been reported (Collenette, 1985) in western south part of Saudi Arabia. The biological activities of some plants growing in Asir region were explored and found it had promising antimicrobial activities (Al Yahya *et al.*, 2018; Mahmoud *et al.*, 2016; Moustafa *et al.*, 2018b; Moustafa *et al.*, 2013).

A. canariense is a succulent, seasonal to short-lived perennial herb with very dense prostrate stems, often used as food and leaves are eaten in famine times (Fern, 2018). Therefore, the aim of this study was to synthesize AgNPs using cold and hot fresh aqueous extract of *A. canariense* leaf parts as reducing agents and characterizing the differences between both extracts using UV-Vis spectroscopy, XRD, SEM and FTIR analyses. The antifungal behavioral activity of these synthesized nanoparticles was investigated towards strains of plant pathogenic microbes namely *Alternaria alternate, Drechslera halodes, Fusarium oxysporum f. sp. lycopersici, Penicillium expansum, Rhizoctonia solani, Pythium ultimum and Macrophomina phaseolina*.

MATERIALS AND METHODS

Preparation of plant extract: 200 gm of *A. canariense* leaf parts were collected in July 2019 from abandoned area in Abha, Asir, Saudi Arabia (18°15'08.6"N; 42°33'05.8"E). Leaf parts of plants washed very thoroughly with distilled water several times to remove any adhered soil particles and then ground into a fine particles using an electric blinder for 5 minutes with the addition 200 mL of distilled water. The sample was filtered with Whatman® qualitative filter paper, Grade 1. 100 mL of the resulted filtrate was boiled at 100°C for fresh hot water extraction and another 100 mL of the filtrates used as it and both solutions were preserved in a polyethylene bag in a refrigerator until further use (Moustafa *et al*. 2020).

Inouclums: Seven fungal strains namely *A. alternate, D. halodes, F. oxysporum f. sp. lycopersici, P. expansum, P. ultimum, R. solani and M. phaseolina* were obtained from the Biology Department, Faculty of Science, King Khalid University, Saudi Arabia. The fungus was cultured at 30°C on potato dextrose agar (PDA) (OXOID, Hampshire, England). Spores of the fungus were collected from cultures on agar plates after 7 days (Broekaert *et al.*, 1997). The concentration of sporangial suspension was estimated using a cell count chamber and adjusted to 2×10^6 spores mL^{-1} (Abril *et al.*, 2008). Fungal spore suspensions have been preserved in 20% glycerol at 4°C for further applications.

***Synthesis of silver nanoparticles (AgNPs)*:** Aqueous solution of 0.5 mM silver nitrate ($AgNO_3$) was prepared using deionized water. First, 9 ml of $AgNO_3$ solution (0.5 mM) was added to 1 ml of leaf extract of *A. canariense*. The reaction was allowed to take place in 20 ml volumetric flasks at 70°C till change the color from dark brown to be blackish to ensure the reduction of $AgNO_3$ by aqueous crude extract. The AgNPs obtained from *A. canariense*-AgNPs were collected by centrifugation at 11,000 rpm for 25 minutes at 25°C (Qais *et al.*, 2019). The formed pellet from each extract was dried in an oven at 60°C for further experimental works.

***Characterization of Nanoparticles Synthesized by A. canariense aqueous extracts*:** *A. canariense*-AgNPs were initially characterized using a UV-visible spectrophotometer by recording the UV-visible spectra of solutions. The absorbance spectra (300–600 nm) of AgNPs solution were monitored using (HITACHI, Model U-2800 spectrophotometer) and distilled water was used as a baseline correction. The AgNPs morphology images were studied via scanning electron microscopy (SEM) (JSM-7500 F; JOEL-Japan). The SMILEVIEW software attached to SEM system was used to obtain the size of AgNPs. The FTIR spectra were recorded over the range of 400–4000 cm^{-1} using The FT-IR with diamond ATR platform spectrometer (Agilent, Cary 630, USA). The crystalline nature, phase identification and grain size had been achieved by XRD (Shimadzu, 6000 Diffractometer, Japan) which was operated at 40 kV and 30 mA using Cu Kα radiations with 1.54 A^0. The average crystallite size corresponding to the observed peaks was

calculated from the Debye–Scherrer relation (Cullity, 1978), $D = (0.9\ \lambda)/(\beta\cos\theta)$, (D is the average size of the crystals, λ is the wavelength of radiation, β is the full width at half the maximum height (FWHM), and θ is the position of the maximum diffraction peak).

In vitro screening of nanoparticles using plate-well diffusion method: The antifungal inhibition activity of synthesized nanoparticles (NPs) from hot and cold aqueous extract of leaf of *A. canariense* was assayed towards *A. alternate, D. halodes, F. oxysporum f. sp. lycopersici, P. expansum, P. ultimum, R. solani and M. phaseolina*, by plate diffusion technique on the growth medium of the PDA (Talibi *et al.*, 2012; Thangavelu *et al.*, 2013). 1000 µL of previously fungal suspension from each strain was spread onto the surface of solidified 20 ml of *potato dextrose agar* (PDA). 6-mm diameter holes were punched in the solidified (PDA) and filled with 100 µl of the previously prepared AgNPs of cold and hot water extracts of *A. canariense* (Moustafa *et al.*, 2013). As control samples for each experiment, *Dimethyl sulfoxide (DMSO)* solution was used at 20% as negative control and Nystatin (10 µg disc) was used as a positive control, then, all plates kept at 30°C for 120 hours. The evaluation of AgNPs antifungal activities was carried out by calculating the diameter of the inhibition of mycelial growth of each fungal strain.

***Data analysis*:** All experiments were performed in a fully randomized design with three replicates for each treatment. The statistical analysis of the results was carried out by the IBM SPSS statistics software for variance analysis using Post hock (One way - ANOVA).

RESULTS

***AgNPs antimicrobial activities from aqueous extracts of A. canariense leaf*:** *In vitro* screening of AgNPs obtained from aqueous extracts of *A. canariense* leaf part showed antifungal activity against *A. alternate, D. halodes, F. oxysporum f. sp. lycopersici, P. expansum, P. ultimum, R. solani and M. phaseolina* (Table 1). All tested AgNPs of hot water extract gave more potent results than that of the cold water extract in the range between 10.17% and 19.85%. Ag nanoparticles of cold water extract exhibit maximum antifungal activity against *P. expansum* (1.55cm), followed by *P. ultimum* (1.54cm), *D. halodes* (1.43cm) and *F. oxysporum f. sp. lycopersici* (1.34cm). The lowest activity found against *M. phaseolina* (1.17cm), *R. solani* (1.21cm) and *A. alternate* (1.31cm). Regarding, AgNPs of hot water extract, the highest level of inhibition was found against *D. halodes* (1.74cm), followed by *P. ultimum* (1.70cm) and the lowest activity against *R. solani* (1.35cm) and *M. phaseolina* (1.33cm). The moderate level of inhibition was observed against *A. alternate, P. expansum and F. oxysporum f. sp. Lycopersici with an inhibition activity between* (1.55and 1.59cm). *A. alternate* was the most sensitive fungal strain to both extracts as the differences was (19.84%), followed by *F. oxysporum* f. sp. *Lycopersici* (16.17%), *M. phaseolina* (13.57%) and *P. expansum* (13.33%). *R. solani*, *D. halodes* and *P. ultimum* were found to be the lowest fungal strains sensitive to AgNPs of cold and hot water extract of *A. canariense* by 11.54%, 11.45% and 10.17% respectively. The effects of positive control (nystatin) as antifungal agent were significantly different from the AgNPs of cold water extract and hot water extract. The Nystatin antifungal activity showed the highest inhibition against *F. oxysporum* f. sp. *lycopersici* (2.35cm) and the lowest against *A. alternate* (2.15cm). The maximum differences of inhibition activity of positive control than AgNPs antifungal activity of cold water and hot water extracts of *A. canariense* was found against *R. solani* by (49.37 and 43.53%) and *M. phaseolina* by (48.89 and 41.94%), respectively. The lowest differences in inhibition activities between positive control and AgNPs from cold and hot water extracts was found against *P. expansum* by 30.28% and 20.99%, respectively and against *P. ultimum* by 30.0% and 22.88%, respectively. The moderate difference was found against *A. alternate*, *D. halodes* and *F. oxysporum* f. sp. *Lycopersici* between (26.86 and 43.10%).

***SEM of synthesized AgNPs*:** Figure 1 (A and B) shows the captured scanning electron microscopy (SEM) images at same magnification for the synthesized AgNPs via cold water and hot water extract of *A. canariense*. It was observed that the synthesized AgNPs from cold water extract are semi spherical (Figure 1A). Figure 1B shows AgNPs from hot

Table 1. *In vitro* antifungal activity of AgNPs from cold and hot water extracts of *A. canariens* leaf

Pathogenic fungi	Mean diameter of zone of inhibition (cm)			
	NPs from cold water extract of *A. canariense*	NPs from hot water extract of *A. canariense*	Nystatin	DMSO
A. alternate	1.31±0.12**	1.57±0.19**	2.15±0.09	NIZ
P. expansum	1.55±0.09**	1.59±0.17**	2.22±0.11	NIZ
D. halodes	1.43±0.06**	1.74±0.07**	2.28±0.13	NIZ
F. oxysporum f. sp. lycopersici	1.34±0.11**	1.55±0.11**	2.35±0.06	NIZ
M. phaseolina	1.17±0.07**	1.33±0.01**	2.29±0.02	NIZ
P. ultimum	1.54±0.09**	1.70±0.07**	2.20±0.10	NIZ
R. solani	1.21±0.09**	1.35±0.07**	2.40±0.08	NIZ

NIZ ; *No inhibition zone* of negative control against each fungus is 0.0 mm. Values are means ± SD; n=3, (*$p \leq 0.05$; **$p \leq 0.01$)

water extract with almost similar type of AgNPs formation with some nanoclusters which were also appears in cold water extract. The SMILEVIEW results found that the average size of AgNPs of cold water was in between 42 and183 nm and for hot water between 29 and 138 nm.

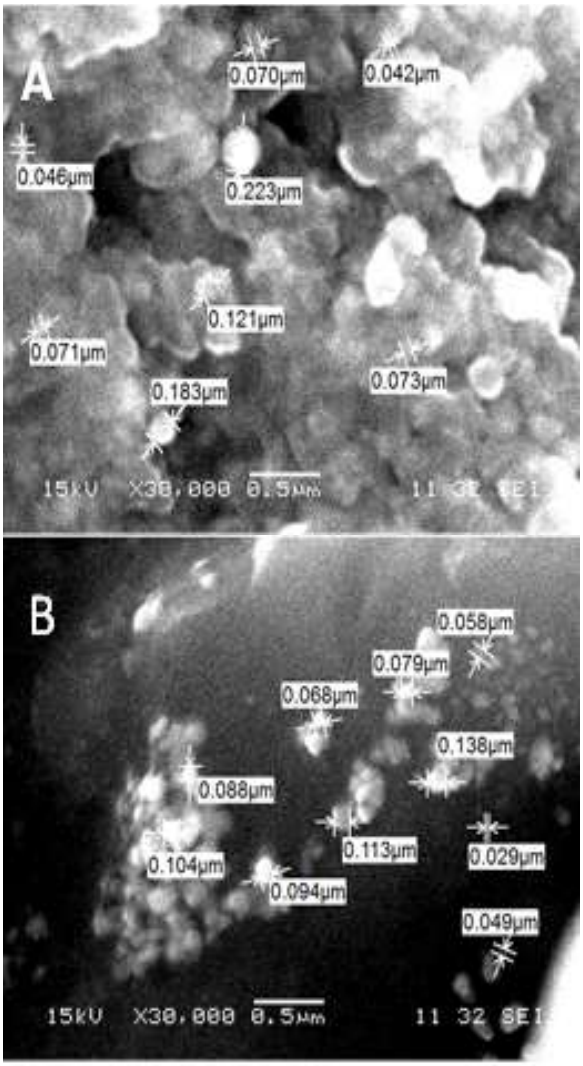

Figure 1. SEM of AgNPs synthesized by cold extract (A) and hot extracts (B) of *A. canariense* leaf.

***FTIR spectroscopy*:** The FTIR spectra of cold water and hot water extracts of *A. canariense* of bioreduction of $AgNO_3$ were shown in (Figure2). The spectrum of cold water extract shows absorption peaks located at 3307, 2927, 1624, 1394, 1250, 1143, 1022, 825, 771 and 513 cm^{-1}. The extract spectrum shows four absorption peaks around 825, 1022, 1143 and 1394 cm^{-1} that can be assigned as the absorption peaks of –C–N stretching vibrations of the amine, –C–O–C or –C–O groups. Similarly, absorption peaks for hot water extract were located at 3355, 2982, 1906, 1631, 1454, 1388, 1310,1260, 1155, 1050, 897, 774, 621 and 440 cm^{-1}. The intense broad peak in the cold water extract spectrum appeared at 3307 cm^{-1} associated with intermolecular hydrogen bonds as a result of -OH group stretching vibrations. Whereas from hot water extract of *A. canariense* extract spectrum, this band is shifted to lower frequency (3355 cm^{-1}) and became much broader with more reaction with Ag^{+} ions.

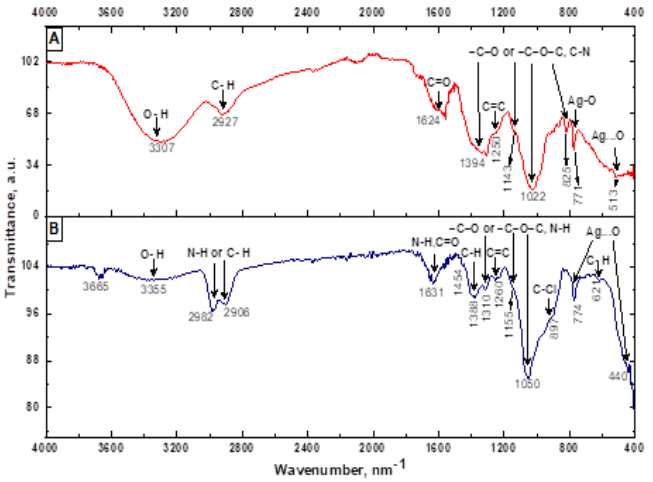

Figure 2. FTIR spectra of AgNPs synthesized by cold extract (A) and hot extracts (B) of *A. canariense* leaf.

***AgNPs UV-Vis spectroscopy*:** Figure 3 shows UV-visible absorption spectra of AgNPs from cold and hot water extract of *A. canariense*. The formation of AgNPs was defined by measuring the surface plasmon resonance (SPR) over the wavelength in range of 200–700 nm. It showed that the broad SPR band peak at 444 nm for AgNPs of cold water extract and 426 nm for hot water extract of *A. canariense.*

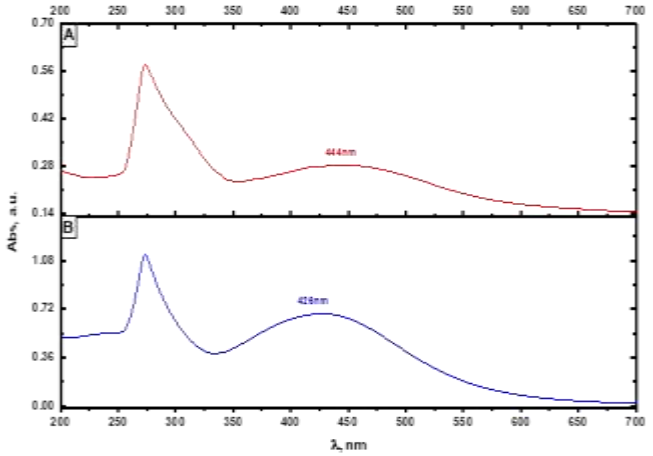

Figure 3. UV-visible absorption spectra of AgNPs synthesized by cold extract (A) and hot extracts (B) of *A. canariense* leaf.

Table 2. XRD data of Ag/AgCl–NPs and Ag/Ag$_2$C2O4 synthesized from cold water extract and hot water extract of *A. canariense* leaf

Sample	Phases	2-theta (in^0)	FHWM	Identified possible h k l planes	Crystallite size (nm)
Cold water extract of *A. canariense*	$Ag_2C_2O_4$	17.38	0.48000	(110)	16.75
		19.10	0.16000	(200)	50.37
	(Silver oxalate)	26.66	0.12000	(-101)	68.07
		28.98	0.27330	(020)	30.04
	JCPDS file:	29.84	0.34600	(011)	23.77
	22-1335	32.37	0.45330	(111)	18.26
		34.98	0.11330	(220)	73.55
		36.48	0.13000	(-301)	52.65
		39.66	0.11500	(-121)	73.47
		46.30	0.32000	(-411)	27.01
		51.76	0.32000	(321)	27.60
		60.09	0.10000	(-312)	91.80
		68.51	0.06000	(431)	160.24
	Ag (Silver)	38.72	0.16000	(111)	52.65
	JCPDS file:	45.04	0.08000	(200)	107.54
	04-0783	65.04	0.09000	(220)	104.71
	Average particles size				12.95
Hot water extracts of *A. canariense*	AgCl	27.91	0.59000	(111)	13.88
	(Silver Chloride)	32.37	0.53600	(200)	15.44
		46.45	0.47000	(220)	18.40
	JCPDS file:	54.77	0.18000	(311)	49.72
	31-1238	57.45	0.18000	(222)	50.35
		66.77	0.22000	(400)	43.26
	Ag (Silver)	38.25	0.41000	(111)	20.52
	JCPDS file:	43.45	0.18000	(200)	47.53
	04-0783	64.83	0.14000	(220)	67.24
	Average particles size				10.83

***AgNPs XRD*:** Figure 4 shows the XRD patterns obtained by green synthesis using plant extracts of cold and hot water of *A. canariense*. In case of extraction by cold water, the phase analysis of obtained XRD pattern indicated 16 peaks out of which 3 peaks matched with Ag with 2θ 38.72°, 45.04° and 65.04° corresponding to JCPDS file: 04-0783. The other major composition was silver oxalate ($C_2Ag_2O_4$) with diffracting angles of 17.38°, 19.10°, 26.66°, 28.98°, 29.84°, 32.37°, 34.98°, 36.48°, 39.66°, 46.30°, 51.76°,60.09 and 68.5° corresponding to JCPDS file:22-1335 (Figure 4A). On the other hand, extraction by hot water, phase analysis of obtained XRD pattern indicated 9 peaks out of which 3 peaks matched with Ag with 2θ 38.25°, 43.45° and 64.83° corresponding to JCPDS file: 04-0783. The other major composition was silver chloride (AgCl) with diffracting angles of 27.91°, 32.37°, 46.45°, 54.77°, 57.45° and 66.77° corresponding to JCPDS file:31-1238 (Figure 4B). Based on the FWHM of the diffraction peaks of synthesized crystals $Ag/Ag_2C_2O_4$ the average nanoparticle size is determined and found 12.95 nm for cold water extraction, and 10.83 nm for hot water (Table 2).

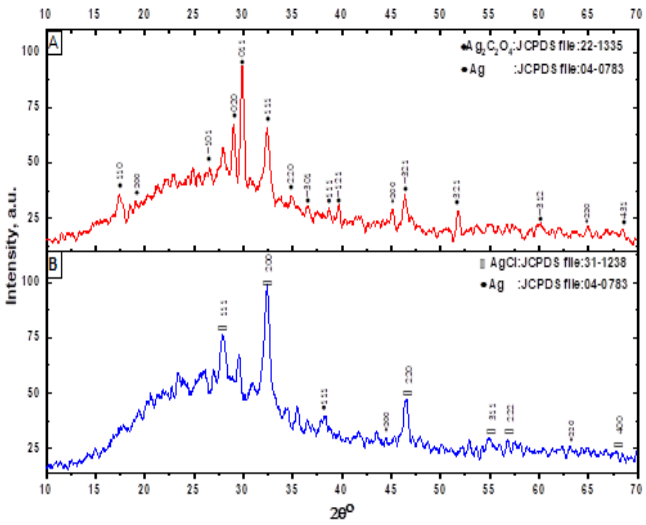

Figure 4. XRD pattern of Ag/AgCl–NPs and Ag/Ag$_2$C$_2$O$_4$ synthesized from cold extract (A) and hot extracts (B) of *A. canariense* leaf.

DISCUSSION

Commonly, FTIR analysis gives information regarding organic and inorganic functional groups involved in the reduction and capping of the metal ions. Herein, both spectrums gained from cold and hot water extracts indicated the existence of the residual plant extract in the prepared AgNPs which acted as capping and reducing agent to the nanoparticles (Prabu and Johnson, 2015). It was reported that the peak at 1631 cm^{-1} is attributed to the carboxyl group (–C=O) stretching vibration (Shameli *et al.*, 2012b). The peaks at 771 and 513 cm^{-1} may be assigned to Ag-NP banding with oxygen (Shameli *et al.*, 2012a). Previous results showed FTIR data greatly affected by proteins in plant specific extract that play crucial role in stability of AgCl-NPs (Hamed *et al.*, 2017). The silver nanoparticles produced are stable and the comparable average size of AgNPs from cold water extract more than those from hot water extract. In addition, these AgNPs showed spectrophotometric absorbance ranged from 426 to 444 nm which is typical characters of these structures (Mallmann *et al.*, 2015). Thus, with the comparison of particles size resulted from two types of plant extracts, it can be concluded that the absorption peak of the Ag-NPs shifted from higher to lower nm i.e. 444 to 426 nm owing to decreased particulate size (Dong *et al.*, 2019; Khan *et al.*, 2013), and the spectra showed changes in either peak intensity or in spectral form (Shameli *et al.*, 2012a).

Results of XRD also support the other obtained data that AgNPs of cold water extract smaller than that of hot water extract. The agglomeration of the formed AgNPs may be due to the influence of the plant extract during the synthesizing process. The results showed that the type of plant extract either cold or hot for the same species plays a key role in the development of fine AgNPs, but the formation of nanoclusters is not preventable due to the preparation of the sample by heating the colloidal solution on the sample holder. However, it was found that plant having chemicals like terpenes, alkaloids amino acids and fatty acids act as a stabilizers agents and prevent the formation of nanoparticles aggregations (Plaza *et al.*, 2010).

With regards to the antifungal activity and in agree with our results it was noted that that small particle size showed high antifungal effect against *Fusarium solani*, *Candida albicans* and *Aspergillus niger* (Yien *et al.*, 2012). Similar studies regarding the impact of synthesized AgNPs from plant extracts on several fungal species have also been recorded (Bahrami-Teimoori *et al.*, 2017; Narayanan and Park, 2014). Several studies have also documented that electrostatic attraction between the negatively charge present on the cell membrane of microorganisms, including fungi, viruses and bacteria and the positively charged nanoparticles is a key rule to the antimicrobial mode of action of nanoparticles (Kim *et al.*, 2007; Xia *et al.*, 2016). It was proposed that silver nanoparticles with wide surface areas could easily form Ag, attach to functional groups (-SH) of proteins and lead in denaturation of protein (Dibrov *et al.*, 2002; Raffi *et al.*, 2008). Silver nanoparticles were found to cause protein degradation and the disruption of the proton pump by binding to the surface proteins of the fungi, raising the permeability of the membrane or protein lipid bilayer and ultimately disrupting the cell membrane (Kim *et al.*, 2009). According to all of the observational, the AgNPs form cold and hot water extract from *A. canariense* were found to be much more effective against the growth of *P. ultimum* and *P. expansum* respectively than other fungal strains. The differences in the susceptibilities of tested fungi to AgNPs from aqueous extract of *A. canariense* most likely due the variations in the chemical composition of the cell wall such as aminopolysaccharides, α- and β-glucans, proteins, lipids, uronic acids, hydrophobins, sporopollenin, and melanins, that protect the cells from stress (Feofilova, 2010).

***Conclusion*:** The present study recorded the green synthesis of AgNPs using *A. canariense* leaf extract which confirmed by XRD, SEM, UV-vis spectroscopy and FTIR analyses. The data presented here demonstrated that AgNPs from *A. canariense* aqueous leaf extract had antifungal activity against various pathogenic plant fungi. Consequently, the findings of this study could be extended to a variety of applications in the field of plant protection. Also, other biological importance such as antiviral, antibacterial and anticancer activities of *A. canariense*-mediated nanoparticles could be also investigated in the future.

***Acknowledgements*:** Thanks to the Deanship of Scientific Research, King Khalid University to fund this article under Research Grant ((R.G.P.1/75/40).

REFERNCES

Abril, M., K.J. Curry, B.J. Smith and D.E. Wedge. 2008. Improved microassays used to test natural product-based and conventional fungicides on plant pathogenic fungi. Plant Dis. 92: 106-112.

Al Yahya, N.A., S.A. Alrumman and M.F. Moustafa. 2018. Phytochemicals and antimicrobial activities of Rumex nervosus natural populations grown in Sarawat Mountains, Kingdom of Saudi Arabia. Arab. J. Sci. Eng. 43: 3465-3476.

Alamri, S.A. and M.F. Moustafa. 2012. Antimicrobial properties of 3 medicinal plants from Saudi Arabia against some clinical isolates of bacteria. Saudi Med. J 33: 272-277.

Alghamdi, S.S.K. 2013. Topical depilatory and method of removing hair. Google Patents.

Bahrami-Teimoori, B., Y. Nikparast, M. Hojatianfar, M. Akhlaghi, R. Ghorbani and H.R. Pourianfar. 2017. Characterisation and antifungal activity of silver

nanoparticles biologically synthesised by *Amaranthus retroflexus* leaf extract. J Exp Nanosci. 12: 129-139.

Broekaert, W.F., B.P. Cammue, M.F. De Bolle, K. Thevissen, G.W. De Samblanx, R.W. Osborn and K. Nielson. 1997. Antimicrobial peptides from plants. Crit. Rev. Plant Sci. 16:297-323.

Clement, J.L. and P.S. Jarrett. 1994. Antibacterial silver. Met.-Based Drugs 1: 467-482.

Collenette, S. 1985. Illustrated guide to the flowers of Saudi ArabiaScorpion, " Scorpion publishing Ltd., London, 1985.

Cullity, B. 1978. ElementsofX-rayDiffraction, 2nd. Addison-Wes1ey, Inc: 332.

Dibrov, P., J. Dzioba, K.K. Gosink and C.C. Häse. 2002. Chemiosmotic mechanism of antimicrobial activity of Ag+ in *Vibrio cholerae*. Antimicrobial agents and chemotherapy 46:2668-2670.

Dong, Y., H. Zhu, Y. Shen, W. Zhang and L. Zhang. 2019. Antibacterial activity of silver nanoparticles of different particle size against Vibrio Natriegens. PloS one 14: e0222322.

Feofilova, E. 2010. The fungal cell wall: modern concepts of its composition and biological function. Microbiology 79:711-720.

Fern, K. 2018. Tropical plants database. Tropicaltheferns. info/viewtropical. php.

Gurunathan, S. 2019. Rapid biological synthesis of silver nanoparticles and their enhanced antibacterial effects against *Escherichia fergusonii* and *Streptococcus mutans*. Arab. J. Chem. 12:168-180.

Hamed, S.M., M.M. Abdel-Alim, N. Abdel-Raouf and I.B. Ibraheem. 2017. Biosynthesis of silver chloride nanoparticles using the cyanobacterium Anabaena variabilis. Life Sci. J. 14:25-30.

Jain, P.K., X. Huang, I.H. El-Sayed and M.A. El-Sayed. 2008. Noble metals on the nanoscale: optical and photothermal properties and some applications in imaging, sensing, biology, and medicine. Acc. Chem. Res. 41:1578-1586.

Jeong, S.H., S.Y. Yeo and S.C. Yi. 2005. The effect of filler particle size on the antibacterial properties of compounded polymer/silver fibers. J. Mater. Sci. 40: 5407-5411.

Jo, Y.-K., B.H. Kim and G. Jung. 2009. Antifungal activity of silver ions and nanoparticles on phytopathogenic fungi. Plant Dis. 93:1037-1043.

Kannan, N., S. Selvaraj and R.V. Murty. 2010. Microbial production of silver nanoparticles. DIG. J. NANOMATER. BIOS. 5:135-140.

Khan, M., M. Khan, S.F. Adil, M.N. Tahir, W. Tremel, H.Z. Alkhathlan, A. Al-Warthan and M.R.H. Siddiqui. 2013. Green synthesis of silver nanoparticles mediated by *Pulicaria glutinosa* extract. Int. J. Nanomedicine 8: 1507.

Kim, J., J. Lee, S. Kwon and S. Jeong. 2009. Preparation of biodegradable polymer/silver nanoparticles composite and its antibacterial efficacy. J. Nanosci. Nanotechnol. 9:1098-1102.

Kim, J.S., E. Kuk, K.N. Yu, J.-H. Kim, S.J. Park, H.J. Lee, S.H. Kim, Y.K. Park, Y.H. Park and C.-Y. Hwang. 2007. Antimicrobial effects of silver nanoparticles. Nanomedicine: NBM 3:95-101.

Kim, S.W., J.H. Jung, K. Lamsal, Y.S. Kim, J.S. Min and Y.S. Lee. 2012. Antifungal effects of silver nanoparticles (AgNPs) against various plant pathogenic fungi. Mycobiology 40:53-58.

Lin, Y.L., W.Y. Wang, Y.H. Kuo and C.F. Chen. 2000. Nonsteroidal constituents from Solanum incanum L. J. Chin. Chem. Soc. 47:247-251.

Magudapathy, P., P. Gangopadhyay, B. Panigrahi, K. Nair and S. Dhara. 2001. Electrical transport studies of Ag nanoclusters embedded in glass matrix. Physica B: Condensed Matter 299:142-146.

Mahmoud, M.F., S.A. Alrumman and A.E.-L. Hesham. 2016. Biological activities of some Acacia spp.(Fabaceae) against new clinical isolates identified by ribosomal RNA gene-based phylogenetic analysis. Pak. J. Pharm Sci. 29(1):221-229.

Mallmann, E.J.J., F.A. Cunha, B.N. Castro, A.M. Maciel, E.A. Menezes and P.B.A. Fechine. 2015. Antifungal activity of silver nanoparticles obtained by green synthesis. Rev. Inst. Med. Trop. São Paulo 57:165-167.

Min, J.S., K.S. Kim, S.W. Kim, J.H. Jung, K. Lamsal, S.B. Kim, M. Jung and Y.S. Lee. 2009. Effects of colloidal silver nanoparticles on sclerotium-forming phytopathogenic fungi. Plant Pathol J. 25:376-380.

Moustafa, M., M. Sayed, S. Alamri, H. Alghamdii and A. Shati, et al., 2020. Pharmaceutical properties of synthesized silver nanoparticles from aqueous extract of *Solanum incanum* L. fruits against some human pathogenic microbes. Int. J. Pharmacol. 16:514-521.

Moustafa, M., S. Alamri, M. Elnouby, T. Taha, M. Abu-Saied, A. Shati, M. Al-Kahtani and S. Alrumman. 2018a. Hydrothermal preparation of TiO 2-Ag nanoparticles and its antimicrobial performance against human pathogenic microbial cells in water. Biocell 42:93.

Moustafa, M., S. Siddiqui, S. Alrumman, A. Shati and M. Al-Kahtani. 2018b. Antimicrobial activity and heavy metals findings of *Euryops arabicus* (Jabur) leaves against plant and human pathogens. Pak. J. Pharm Sci. 55:787-792.

Moustafa, M.F., S.A. Alamri, T.H. Taha and S.A. Alrumman. 2013. In vitro antifungal activity of *Argemone ochroleuca* Sweet latex against some pathogenic fungi. Afr. J. Biotechnol. 12:1132-1137.

Narayanan, K.B. and H.H. Park. 2014. Antifungal activity of silver nanoparticles synthesized using turnip leaf extract (*Brassica rapa* L.) against wood rotting pathogens. Eur. J. Plant Pathol. 140:185-192.

Park, H.-J., S.-H. Kim, H.-J. Kim and S.-H. Choi. 2006. A new composition of nanosized silica-silver for control of various plant diseases. Plant Pathol. J. 22: 295-302.

Plaza, M., S. Santoyo, L. Jaime, G.G.-B. Reina, M. Herrero, F.J. Señoráns and E. Ibáñez. 2010. Screening for bioactive compounds from algae. J. Pharm. Biomed. 51:450-455.

Prabu, H.J. and I. Johnson. 2015. Plant-mediated biosynthesis and characterization of silver nanoparticles by leaf extracts of *Tragia involucrata*, *Cymbopogon citronella*, *Solanum verbascifolium* and *Tylophora ovata*. Karbala Int. J. Mod. Sci. 1:237-246.

Qais, F.A., A. Shafiq, H.M. Khan, F.M. Husain, R.A. Khan, B. Alenazi, A. Alsalme and I. Ahmad. 2019. Antibacterial effect of silver nanoparticles synthesized using *Murraya koenigii* (L.) against multidrug-resistant pathogens. Bioinorg. Chem. Appl. 2019:1-11.

Raffi, M., F. Hussain, T. Bhatti, J. Akhter, A. Hameed and M. Hasan. 2008. Antibacterial characterization of silver nanoparticles against *E. coli* ATCC-15224. J Mater Sci Technol. 24: 192-196.

Salomoni, R., P. Léo, A. Montemor, B. Rinaldi and M. Rodrigues. 2017. Antibacterial effect of silver nanoparticles in *Pseudomonas aeruginosa*. Nanotechnol Sci Appl. 10:115-121.

Shameli, K., M.B. Ahmad, S.D. Jazayeri, P. Shabanzadeh, P. Sangpour, H. Jahangirian and Y. Gharayebi. 2012a. Investigation of antibacterial properties silver nanoparticles prepared via green method. Chem. Cent. J. 6:73.

Shameli, K., M. Bin Ahmad, E.A. Jaffar Al-Mulla, N.A. Ibrahim, P. Shabanzadeh, A. Rustaiyan, Y. Abdollahi, S. Bagheri, S. Abdolmohammadi and M.S. Usman. 2012b. Green biosynthesis of silver nanoparticles using *Callicarpa maingayi* stem bark extraction. Molecules 17: 8506-8517.

Shenashen, M.A., S.A. El-Safty and E.A. Elshehy. 2014. Synthesis, morphological control, and properties of silver nanoparticles in potential applications. PART PART SYST CHAR. 31:293-316.

Talibi, I., L. Askarne, H. Boubaker, E. Boudyach, F. Msanda, B. Saadi and A.A.B. Aoumar. 2012. Antifungal activity of some Moroccan plants against *Geotrichum candidum*, the causal agent of postharvest citrus sour rot. Crop Prot. 35:41-46.

Thangavelu, R., P.G. Devi, M. Gopi and M. Mustaffa. 2013. Management of Eumusae leaf spot disease of banana caused by *Mycosphaerella eumusae* with Zimmu (*Allium sativum*× *Allium cepa*) leaf extract. Crop Prot. 46:100-105.

Valli, J.S. and B. Vaseeharan. 2012. Biosynthesis of silver nanoparticles by *Cissus quadrangularis* extracts. Mater. Lett. 82:171-173.

Xia, Z.-K., Q.-H. Ma, S.-Y. Li, D.-Q. Zhang, L. Cong, Y.-L. Tian and R.-Y. Yang. 2016. The antifungal effect of silver nanoparticles on *Trichosporon asahii*. J Microbiol Immunol Infect. 49:182-188.

Yien, L., N.M. Zin, A. Sarwar and H. Katas. 2012. Antifungal activity of chitosan nanoparticles and correlation with their physical properties. Int J Biomater. 2012:1-9.